Project 3: Analysis of Airfoils Using the Vortex Panel Method

ME 163: Engineering Aerodynamics

Sebastian Baehr

15 April 2021

Abstract

This project aims to examine the performance of the symmetric NACA 0012 and asymmetric NACA 4412 airfoils. Properties under examination include the pressure coefficient distributions, lift coefficients, and stall angles for each airfoil. Knowing these parameters sets up the necessary steps to fully examine the performance of each airfoil and determine whether it meets the required design objectives. For pressure distributions, plots of the distributions of the upper and lower surfaces were created for each airfoil at angle of attacks 16°, 8°, -8°, and -16°. For the lift coefficients, a plot was created for each airfoil that displayed the lift coefficient vs angle of attack curve for the -16° to 16°, and compared this curve to the analytical solution. Lastly, using the same angle of attack range, a plot of the flow separation point vs angle of attack was created in order to determine the what angle of attack was the stall angle, and compared that to experimentally determined stall angles. It was determined that the numerical and analytical models for lift coefficients had relatively good agreement, while that stall angles determined numerically did not agree very well with the experimentally found stall angles.

Formulation

To calculate the pressure coefficient distributions and the separation points for each airfoil, I used the same formulaic methods of the vortex panel method and Thwaites's condition, respectively, that was outlined in the project 2 report. For the purpose of space, I will not outline the equations of these methods here, but refer you to the project 2 report.

Two different methods were used to calculate the lift coefficients. The first, was a numerical method that utilized the pressure coefficients to determine the net lift force of each airfoil. To begin the pressure coefficients C_p at each point$i$ along the airfoil surface determined earlier were converted into actual pressures P (Eq. 1). From these pressures, the net lift force$L$ of the airfoil was determined (Eq. 2). Lastly, the net lift force was used to determine the coefficient of lift C_L (Eq. 3).

$$P(i) = \frac{1}{2} C_p(i) \rho U_\infty^2 + P_\infty \tag{1}$$

$$F = (D, L) = \int -P\hat{\boldsymbol{n}}\, dA \tag{2}$$

$$C_L = \frac{L}{\frac{1}{2}\rho U_\infty^2 c} \tag{3}$$

Here ρ is the density of air taken at 1.225 kg/m^3, U_∞ is the relative freestream air velocity set at 25 m/s, $\hat{\boldsymbol{n}}$ is the directional vectors in tangent and normal top the airfoil surface, and c is the chord length.

For the analytical model, two different methods were used. For the NACA 0012 airfoil, (Eq. 4) was used were α is the angle of attack. This was done since Thin Airfoil Theory is able to model a symmetric airfoil well. For the NACA 4412 airfoil, (Eq. 5) was used where α_{L_0} is the zero-lift angle and taken to be -4.15° for the NACA 4412.

$$C_L = 2\pi\alpha \tag{4}$$

$$C_L = 2\pi(\alpha - \alpha_{L_0}) \tag{5}$$

Lastly, in order to determine the stall angle of each airfoil, the criterion of when the upper surface separation point was within 20% of the length of the chord from the leading edge was used. Once the separation point was within this 20%, the airfoil was considered to be in stall. Thus, finding the angle for the separation point crossed the 20% threshold yielded the stall angle.

Implementation

To start, the geometry of the NACA 0012 and 4412 was imported into MATLAB were control points and panel lengths were then calculated. The geometry was then imported into the same main code I used for project 2 so that the pressure coefficient distribution and separation points could be calculated. Then I added to my main code script the structure to calculate the lift force from each vortex panel. I then summed them up to find the total lifting force, and numerically calculate the lift coefficient. Finally, I added code in order to perform (Eq. 5) to get the lift coefficient analytically.

In order to sweep through the angle of attack range in order to generate the lift coefficient and separation point plots, I created another script that called the main code script for every 0.1° angle increment between -16° to 16°. To find the stall angle, I found the two angles where one had a separation point farther than 20% of the chord length from the leading edge, and one had a separation point closer than 20% of the chord length from the leading edge, and the used linear interpolation to find the exact angle where the separation point was 20% of the chord length from the leading edge.

Results

The pressure coefficient distribution for the upper and lower surfaces of each airfoil are shown in Figure 1. It is evident from the plots that when the angle is negative, the upper surface has positive pressure coefficients, and the lower surface has negative pressure coefficients. When the angle of attack is positive, the opposite is true. This demonstrates the practicality of having a positive angle of attack for plane wings. Thus, I will now only discuss the results when angle of attack is positive. The plots also demonstrate that positive angle of attacks, the magnitude of the pressure coefficients is much larger that of the bottom surface, allowing for a net lift upward. The rate of increase of the pressure coefficient is much larger along the upper surface than the rate of decrease on the lower surface. and if the angle of attack increases, so does the rate of increase of the upper surface pressure coefficient.

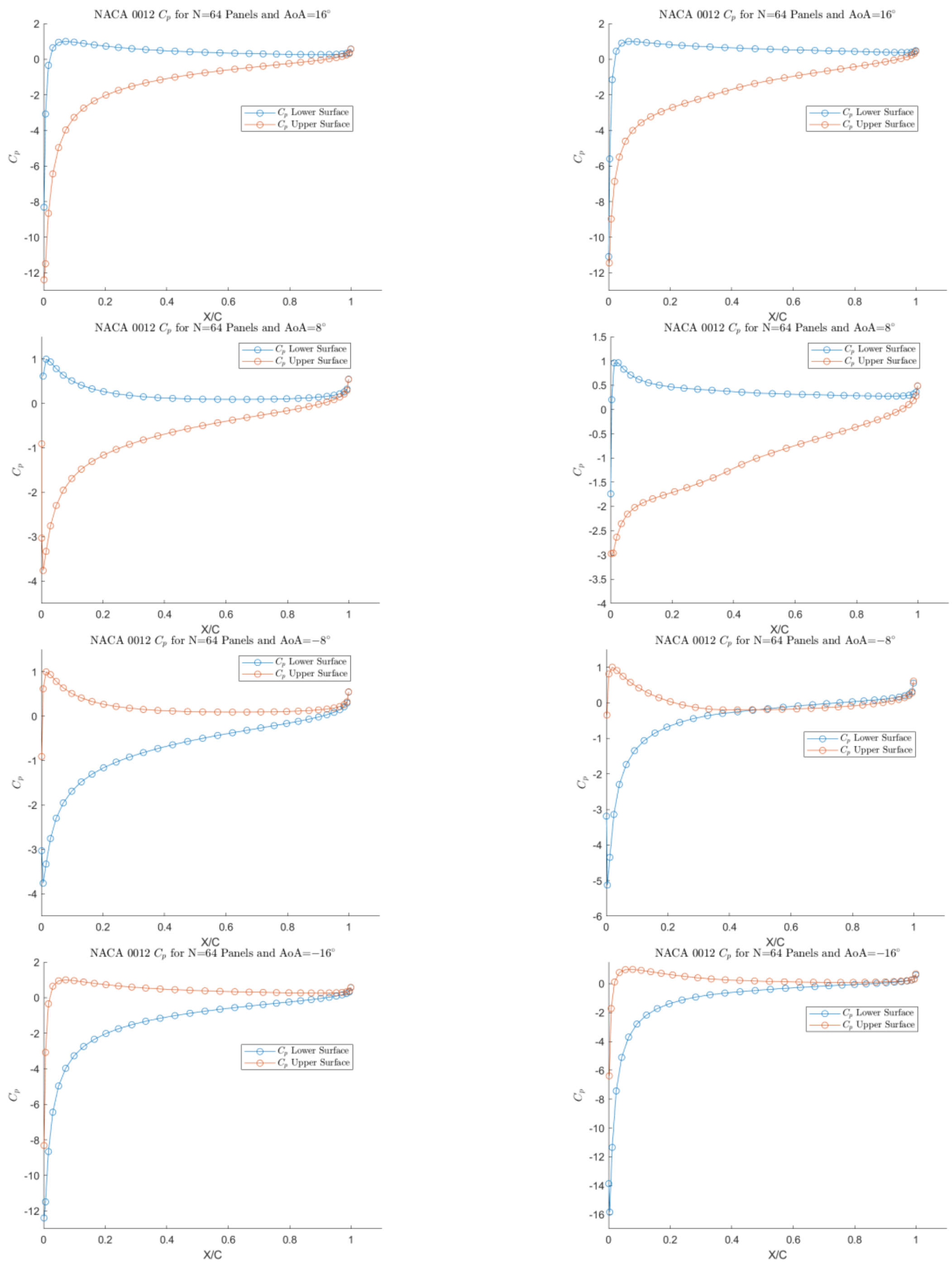

Figure 1: Pressure Coefficient Plots for NACA 0012 (Left) and 4412 (Right) at Angle of Attacks of 16°, 8°, -8°, and -16°

In Figure 2, the numerically calculated lift coefficients are compared to the analytically calculated lift coefficients. In both cases the agreement between the two methods is relatively decent. However, it is apparent that as the magnitude of the angle of attack increases, the disparity between the two methods decreases. This is because for Thin Airfoil Theory, the model becomes less reliable since at high angle of attack, more laminar flow is present. Since Thin Airfoil Theory relies on higher velocity speeds, and more turbulent flow, the more laminar flow present, the more the analytical model will deviate from the actual values.

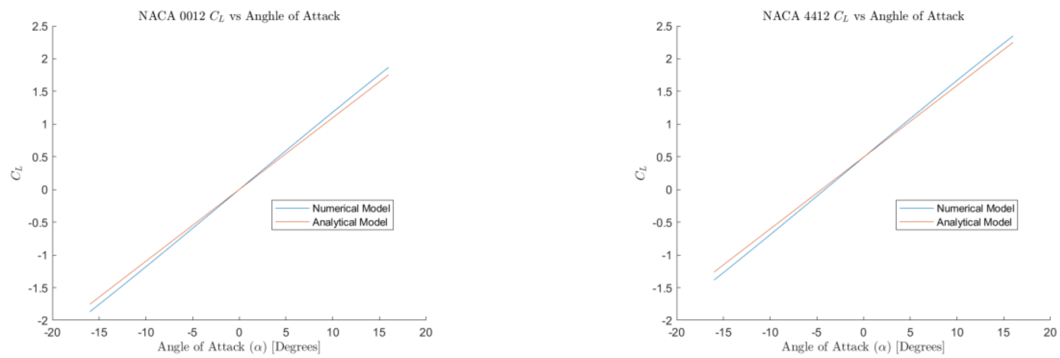

Figure 2: Curves of Lift Coefficients vs Angle of Attacks in range -16° < α < 16°

When comparing the plots in Figure 2 to the lift coefficient plots presented in Abbott's *Theory of Wing Sections* from experiments, the lift coefficients for both airfoils presented here fairly at most angles of attack. At higher angles of attack, deviation become somewhat larger. Again, this is because using Thin Airfoil Theory is not insanely accurate for situations with more laminar and viscous flow, as explained earlier.

In figure 2, the separation point locations expressed as a percentage of the chord length vs angle of attack curve is plotted for each airfoil. Along with that is a horizontal line at 20% to mark the stall angle criterion described earlier. From the plots, the stall angle for each airfoil was determined and displayed in Table 1. The movement of the stagnation point towards the leading edge as the angle of attack increases is explained by the facts that came from the pressure distribution plots. Since the pressure coefficient increases at a faster rate at higher angle of attacks, separation becomes more viable as it causes deceleration of flow and thus will happen sooner along the upper surface of the airfoil. Comparing the stall angles calculated using the 20% criterion, and those determined from experiment in other literature, it is apparent that there is a large discrepancy between the methods. This is most likely due to our separation points being based on a model where viscous and laminar flow is not modelled well.

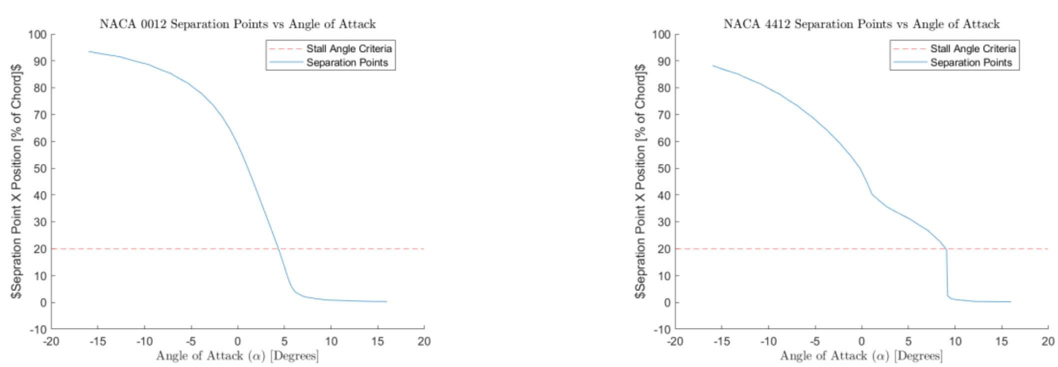

Figure 2: Curves of Separation Points vs Angle of Attacks in range -16° < α < 16°
With Stall Angle Criteria Reference

Table 1: Stall Angles for NACA 0012/4412 Airfoils

Airfoil	Stall Angle Using Criteria [Degrees]	Stall Angle Experimental [Degrees]
NACA 0012	4.35	~14.00
NACA 4412	9.01	~16.00